NOAA Technical Report ERL 387–WPL 50

Feasibility of Monitoring Aerosol Concentrations by 10.6-μm Backscatter Lidar

Gordon Lerfald

May 1977

U.S. DEPARTMENT OF COMMERCE
National Oceanic and Atmospheric Administration
Environmental Laboratories

NOAA Technical Report ERL 387–WPL 50

Feasibility of Monitoring Aerosol Concentrations By 10.6-μm Backscatter Lidar

Gordon Lerfald

Wave Propagation Laboratory
Boulder, Colorado

May 1977

U.S. DEPARTMENT OF COMMERCE
Juanita Kreps, Secretary

National Oceanic and Atmospheric Administration
Robert M. White, Administrator

Environmental Research Laboratories
Wilmot Hess, Director

Contents

Feasibility of Monitoring Aerosol Concentrations By 10.6-μm Backscatter Lidar

Gordon Lerfald

ABSTRACT. The feasibility of remotely monitoring aerosol concentrations by means of backscatter lidar systems operating at the wavelength 10.6 μm was investigated by experimental tests and calculations. A prototype lidar system was built and was operated in conjunction with equipment that permitted direct measurement of particle size distribution of aerosols in essentially the same sampled volume. The backscattered signals measured by the test system agreed to within a factor of two with the backscatter computed from the measured particle size distributions. The experimental results are used to predict the performance of systems having transmitter powers and receiver collecting optics different from those used for the test system.

1. Introduction

The relatively high transparency of the atmosphere in the 8–13-μm infrared "window" and recent development of high power lasers in this wavelength range lead to interesting possibilities for remote sensing systems. Backscatter Doppler lidar systems using 10.6-μm CO_2 lasers have been described by Huffaker (1974) and by Schwiesow and Cupp (1976). This report describes results obtained from a non-Doppler test system that included a 10-W, 10.6-μm, CO_2, CW laser transmitter, and a radiometer-type receiver.

A potential application of 10-μm backscatter lidar is vertical probing of the atmosphere in urban areas to determine the loading of particulate pollutants. The test arrangement was designed with such an application in mind. By measuring the vertical distribution of aerosols, temperature inversions may be detected and the thickness of the boundary layer determined approximately. Detection of cloud base heights by a similar lidar system has not been demonstrated, but is almost certainly feasible. The primary objective of the work was to obtain data from which to estimate the capabilities of proposed 10-μm backscatter lidar systems. The approach used was to compare measured backscattered power with power computed from known aerosol distributions.

2. Description of the Lidar Test System

The physical configuration used was that of an "intersecting beam" system, with separate laser transmitter and receiver and with a steering mirror displaced at an appropriate baseline distance. Rotation of the mirror sweeps the transmitted beam in the plane of the receiver beam to provide a range sweep. This type of system could be quite easily automated for unattended operation at a stationary site. The mountings for receiver and transmitter would have to be rigid and the mirror mount of high precision. This geometry is routinely used in operational rotating beam ceilometers by the National Weather Service.

The components (Fig. 1) were assembled on a sturdy mounting. A 10-cm diameter, f/4.0, reflecting telescope collected the backscattered signal, and germanium lenses focused the signal onto a mercury-cadmium-tellurium detector, cooled by liquid nitrogen.

The transmitted laser beam was chopped at a frequency of 100 Hz. The received signal was processed by a commercial phase-lock amplifier synchronized by the chopper reference. An integrating time constant of either 1 or 3 seconds was normally used.

A clock-driven shutter periodically interrupted the transmitted laser beam to provide calibration levels. The recorded signal could then be visually averaged during the data collection and calibration periods respectively. Figure 2 shows an example of the data obtained.

The noise equivalent power (NEP) of the detector is about 1×10^{-13} W/Hz$^{\frac{1}{2}}$. However, the output signal evidenced low-frequency, random fluctuations (characteristic time constants about 5–50 sec), with amplitude several times as much as this noise. Various system checks indicated that these variations were due to small fluctuations in the temperature of the cooled detector.

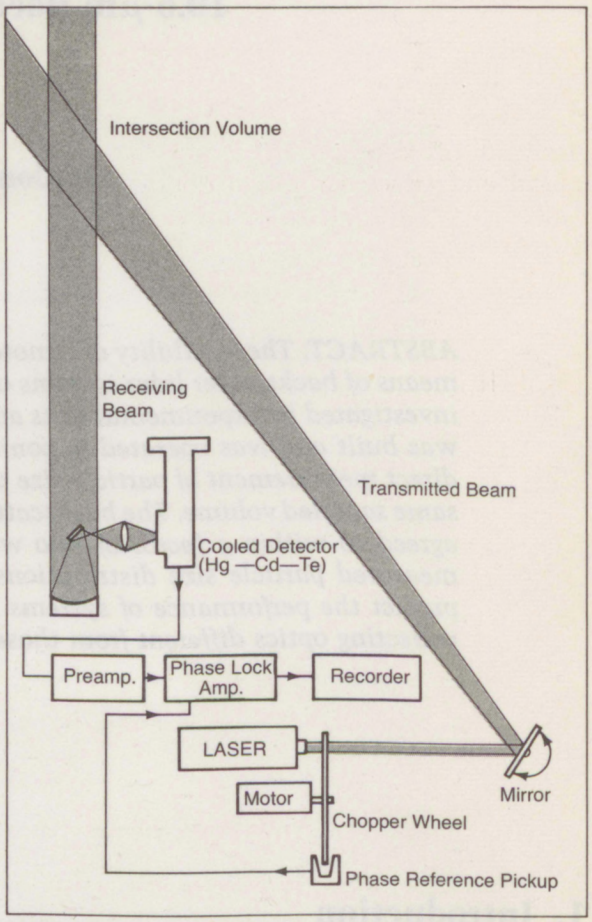

Figure 1. Schematic representation of intersecting beam lidar system.

The greatest constraint on the efficiency of the test system was a mismatch between the angular divergence of the laser transmitter beam and the telescope field of view. The latter was limited by the size of the detector element and the field of view (fov) of the receiver optics to about 1 mrad, while the transmitter beam width was about 3 mrad. Collimation of the transmitter beam would have solved the problem but considerations of cost and delivery time led us to try the experiment without a collimator. Computations showed that the system had an optical collection efficiency of approximately 10 percent under these conditions.

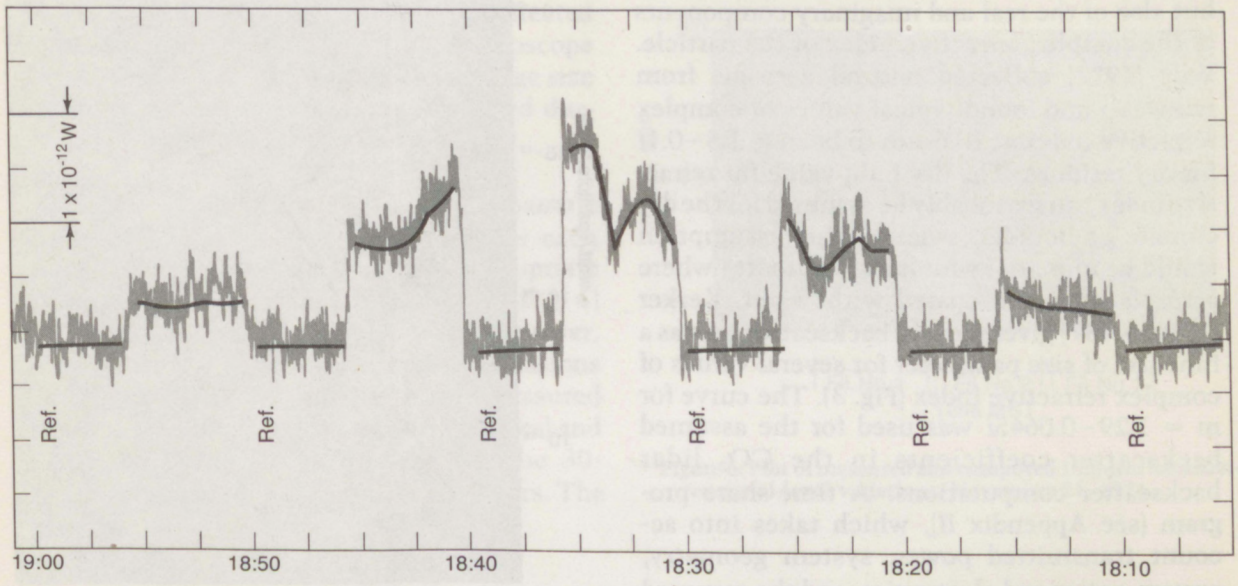

Figure 2. Sample chart record of 10.6-μm lidar backscatter. This shows the variations in aerosol backscatter as a function of time. The transmitter beam is interrupted during intervals labeled "Ref."

3. Observations

The equipment was first tested in the laboratory with the laser and telescope beams directed out a window. Small, polished steel spheres were used for alignment of the beams and to obtain system calibrations. (The calibration method is described in Appendix I.) The intersection volume was about 1 liter, with the intersection center approximately 20 m from the equipment. For convenience of calibration the intersection volume was about 2 m above ground level. Measurable backscatter signal was observed sporadically, usually when visible haze was also observable.

It was decided to compare lidar backscatter power with data taken by the Atmospheric Physics and Chemistry Laboratory (APCL) of NOAA, and the lidar was set up in a trailer adjacent to the APCL facility for simultaneous observations. On November 21, and again on November 27, 1974, coordinated sets of measurements, including filter discs, were obtained with APCL. These data were analyzed to obtain direct comparisons of the observed 10.6-μm backscatter signal and computed backscatter due to measured particle size distributions.

4. Backscatter Gain

The greatest diffculty in estimating the performance of a 10.6-μm lidar system by calculation appeared to lie in the lack of definite knowledge of the backscatter gain appropriate for aerosol particles.

The backscatter gain for atmospheric aerosols is a function not only of particle size but also of the real and imaginary components of the complex refractive index of the particle. Volz (1972) collected natural aerosols from rainwater and found typical values of complex refractive index at 10.6-μm to be $m = 1.5-0.1i$ for dry residues. The dry bulk value for refractive index can reasonably be assumed for the dry climate at Boulder, whereas this assumption would be more risky for humid climates where aerosols often are coated with water. Kerker (1969, p. 137) gives plots of backscatter gain as a function of size parameter for several values of complex refractive index (Fig. 3). The curve for $m = 1.29-0.0645i$ was used for the assumed backscatter coefficients in the CO_2 lidar backscatter computations. A time-share program (see Appendix II), which takes into account transmitted power, system geometry, system optics and electronics, and the assumed particle characteristics, was used to compute the anticipated backscatter power received by the prototype system for a particle concentration of one per cm^3 for the assumed particle sizes. Results of these computations are shown in Figure 4.

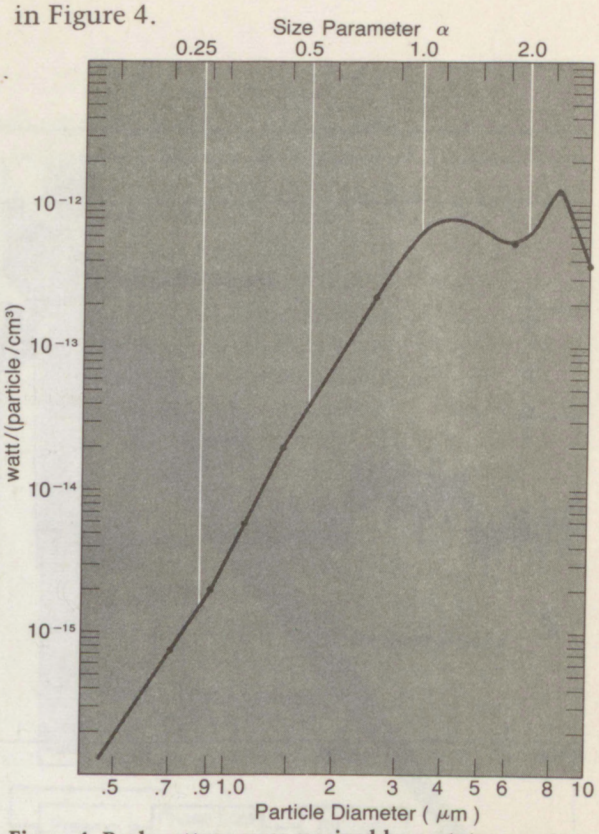

Figure 4. Backscatter power received by prototype system for unit particle concentration (one particle per cm^3), as a function of particle diameter.

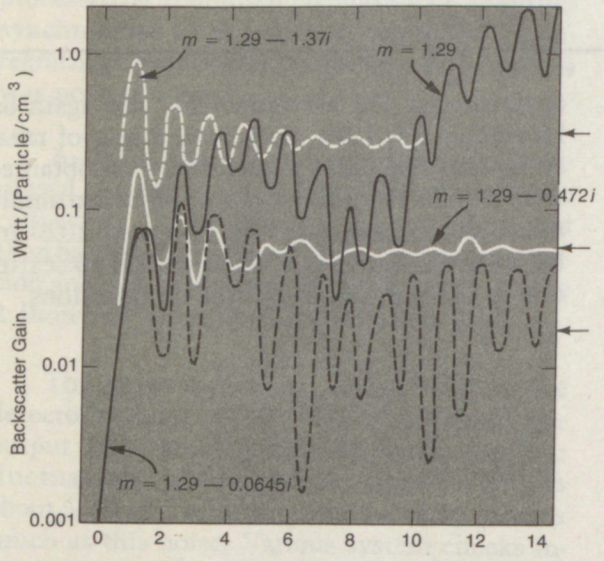

Figure 3. Backscatter gain curves for various values of absorption index (Kerker, 1969, p. 137). The size parameter $\alpha=\pi D/\lambda$, where D is particle diameter.

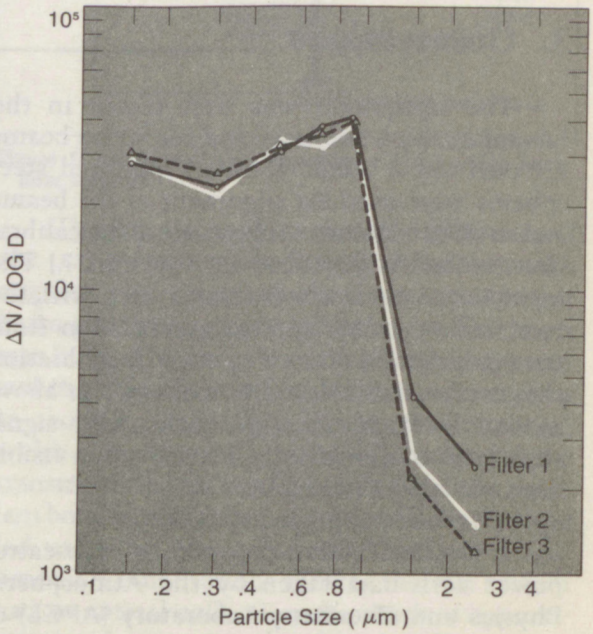

Figure 5. Particle distribution read from APCL filters exposed November 21, 1974. The vertical scale is the number of particles per liter for each range increment in particle size (diameter).

5. Lidar-Filter Comparisons of November 21, 1974

On November 21, 1974, data were collected by the 10.6-μm lidar system while a series of three APCL filters were exposed for 30 minutes each. These 0.1-μm-mesh filters had outside air drawn through them at a rate of approximately 33 liters per minute through an intake mounted about 5 ft above ground. The samples collected were analyzed with an electron microscope (Pueschel et al., 1975) to obtain the average size distribution of aerosol particles collected during the 30-minute exposure periods.

Figure 5 shows the results of the sample analyses. The particle concentration for each size range was multiplied by the appropriate normalized system backscatter power (Fig. 4) and summed to obtain calculated signal power. The data used and the results of the calculations are given in Table 1. Figure 6 plots the measured lidar backscatter signal (5-minute averages) and calculated backscatter levels during the 30-minute exposure times of the APCL filters. The computed values are approximately a factor of 2 lower than the measured values. However, the ratios of the averages of measured values to the computed values are nearly constant (2.3:1, 2.0:1, 2.0:1), for each of the three filter intervals.

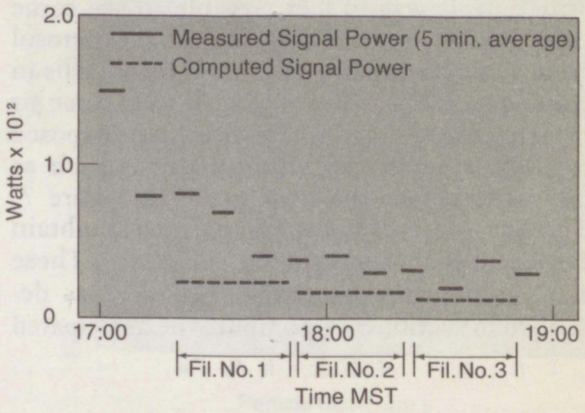

Figure 6. Plot of measured and computed 10.6-μm backscatter signal level variations, November 21, 1974.

Table 1. Data from Filter Samples and Backscatter Signals Computed With Data for November 21

Size Range (μm)	Particle Concentration (part/cm^3)	Backscatter Coefficient (W/part/cm^3)$^{-1}$		Computed Signal (W)
	Filter Sample 1 17:18–17:48 MST November 21, 1974			
0.4–0.6	10	2×10^{-16}		2.0×10^{-15}
0.6–0.8	9.5	7.5×10^{-16}		7.1×10^{-15}
0.8–1.0	8.2	2×10^{-15}		1.6×10^{-14}
1.0–2.0	2.1	2.3×10^{-14}		4.8×10^{-14}
2.0–3.0	0.8	2.0×0^{-13}		1.6×10^{-13}
			Total	2.3×10^{-13}
	Filter Sample 2 17:52–18:21 MST November 21, 1974			
0.4–0.6	12	2×10^{-16}		2.4×10^{-15}
0.6–0.8	8.0	7.5×10^{-16}		6.0×10^{-15}
0.8–1.0	7.8	2×10^{-15}		1.6×10^{-14}
1.0–2.0	1.3	2.3×10^{-14}		3.0×10^{-14}
2.0–3.0	0.5	2.0×10^{-13}		1.0×10^{-13}
			Total	1.5×10^{-13}
	Filter Sample 3 18:25–18:55 MST November 21, 1974			
0.4–0.6	10	2×10^{-16}		2.0×10^{-15}
0.6–0.8	8.7	7.5×10^{-16}		6.5×10^{-16}
0.8–1.0	7.7	2×10^{-15}		1.5×10^{-14}
1.0–2.0	1.1	2.3×10^{-14}		2.5×10^{-14}
2.0–3.0	0.4	2.0×10^{-13}		8.0×10^{-14}
			Total	1.3×10^{-13}

6. Lidar-Filter Comparisons of November 27, 1974

Coordinated measurements with the APCL filters and the 10.6-μm lidar were obtained on November 27, 1974. Figure 7 shows the recorded lidar backscatter signal levels from 14:30 to 21:30. The period 15:30–17:00 was characterized by large fluctuations in the backscatter due to variations in aerosol construction. It was in fact possible to see some evidence of spatial structure in the aerosol clouds by viewing them against the foothills in the distance. Six sets of APCL filters at three air intake rates (1, 5, and 10 liter/min) were exposed for approximately 58-minute periods each as indicated below the time scale of Figure 7. Three of these filters were analyzed to obtain the size distributions shown in Figure 8. These size distribution data were then used as described in section 5, to compute the anticipated signal for the prototype lidar system. Table 2 shows the numerical values used and the computed signals resulting. The total signal power computed is shown in Figure 7. The computed signal in each of the three intervals is somewhat larger than the average measured signal.

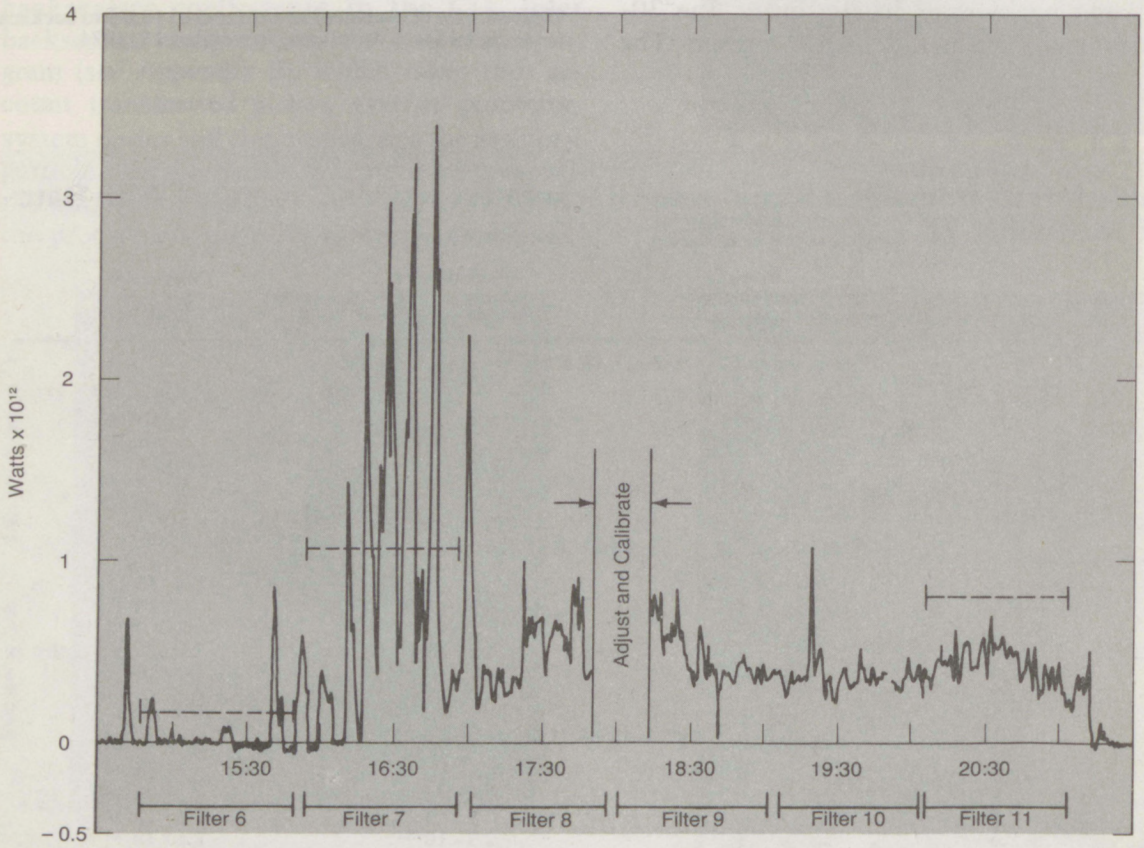

Figure 7. 10.6-μm lidar backscatter signal measured on November 27, 1974 (solid line), and computed backscatter (dashed lines).

7. Discussion

The experiment compared results of the 10.6-μm lidar measurements with the backscatter intensities computed using aerosol particle concentrations obtained from APCL filter analyses.

The measured backscatter signal was approximately half as large as the computed backscatter for November 27, whereas for November 21 the measured values were somewhat larger than the computed backscatter. We do not believe this discrepancy is entirely attributable to experimental errors. The overall system sensitivity was determined during each measurement period and its value was repeatable to ±25%. The calibration was performed by means of a small spherical reflector placed at the point of maximum response in the intersection volume of the transmitter and receiver beams. One possible cause of the discrepancies between measured and computed backscatter intensities is a difference between the actual

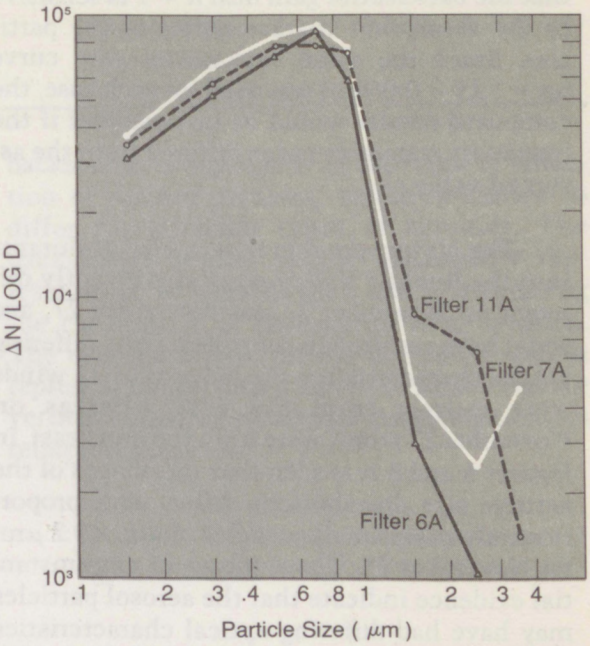

Figure 8. Particle size distribution read from APCL filters exposed November 27, 1974.

Table 2. Data from Filter Samples and Backscatter Signals Computed With Data for November 27

Size Range (μm)	Particle Concentration (part/cm^3)		Backscatter Coefficient (W/part/cm^3)	Computed Signal (W)
	FILTER 6A November 21, 1974 14:50–15:48 MST			
0.4–0.6	71	24	2×10^{-16}	4.8×10^{-15}
0.6–0.8	88	22	7.5×10^{-16}	1.7×10^{-14}
0.8–1.0	56	12	2×10^{-15}	2.4×10^{-14}
1.0–2.0	3.1	1.5	2.3×10^{-14}	3.5×10^{-14}
2.0–3.0	1.0	0.34	2×10^{-13}	6.8×10^{-14}
			Total	1.5×10^{-13}
	FILTER 7A November 27, 1974 15:50–16:48 MST			
0.4–0.6	84	28	2×10^{-16}	5.6×10^{-15}
0.6–0.8	90	22	7.5×10^{-16}	1.7×10^{-14}
0.8–1.0	77	16	2×10^{-15}	3.2×10^{-14}
1.0–2.0	4.8	2.4	2.3×10^{-14}	5.5×10^{-14}
2.0–3.0	2.6	0.85	2.0×10^{-13}	1.7×10^{-13}
3.0–4.0	4.8	1.2	6.5×10^{-13}	7.8×10^{-13}
			Total	1.06×10^{-12}
	FILTER 11A November 27, 1974 20:06–21:04			
0.4–0.6	79	26	2×10^{-16}	5.2×10^{-15}
0.6–0.8	79	20	7.5×10^{-16}	1.5×10^{-14}
0.8–1.0	76	15	2×10^{-15}	3.0×10^{-14}
1.0–2.0	8.8	4.4	2.3×10^{-14}	1.0×10^{-13}
2.0–3.0	6.3	2.1	2.0×10^{-13}	4.2×10^{-13}
3.0–4.0	1.4	0.35	6.5×10^{-13}	2.3×10^{-13}
			Total	8.0×10^{-13}

and the assumed backscatter gain for the particles involved in the two cases. Figure 3 shows that the backscatter gain near $\alpha = 1$ is sensitive to the absorption characteristics of the particles. Since the same backscatter gain curve ($m = 1.29 - 0.0645i$) was used for each case, the computed results would be inconsistent if the imaginary refractive index differed from the assumed value.

The air movements that carried pollutants into the Boulder Valley were significantly different on November 21 and November 27, and could have resulted in aerosols having differing optical characteristics. On November 21 winds were mostly from the east whereas on November 27 winds were from the northeast. In Figures 5 and 8 it is seen that the shapes of the particle size distributions differ, with proportionately more small particles (diam. <0.2 μm) on November 21. These pieces of circumstantial evidence indicate that the aerosol particles may have had differing optical characteristics on the two days in question, although it does not seem possible to prove that this accounts for the differences in the observed and calculated results.

The sensitivity of the prototype lidar was too low to give readable signals on all occasions. The system efficiency could have been increased by approximately a factor of ten by using a suitable collimator on the laser transmitters. Comparisons between particle distributions measured on the APCL filters exposed during pollution events and those exposed during "clear air" conditions showed that the concentration of particles in clear air was less than a factor of ten below that needed for an observable lidar return. It follows that a small CO_2 lidar system (10-watt CW transmitter, 10-cm-diameter collecting optics) is capable of making continuous measurements of aerosol concentration out to at least 60 meters.

8. Estimates of Vertical Sounding Capability

The system's measurements appear to agree with calculations well enough that they can serve as a base for extrapolation to systems having other parameters. Such extrapolations were performed for the case of the vertically directed crossed beam configuration for clear air conditions. The extrapolations assumed an aerosol concentration and size distribution that is the average of several APCL filter measurements taken at Boulder, Colorado, under clear air conditions in May 1974. This distribution is approximately flat at 2×10^4 particles per liter for particles in the size range 0.4 to 1.0 μm and falls off exponentially for particle sizes above 1.0 μm, reaching 2×10^2 particles per liter for 5.0-μm-diameter particles. Further, following McClatchey et al. (1971), it was assumed that the aerosol concentration falls off linearly by a factor of two for each kilometer increase in height.

Extrapolations were made to other laser powers and to other collecting telescope sizes. The height to which backscatter from clear air aerosols could be measured was computed on several height resolutions (maximum dimension of intersection volume at maximum range). The extrapolations, given in Table 3, are believed to be conservative estimates of the range capabilities for vertical sounding of aerosol concentration by 10.6-μm lidar systems. Here, 30-second time averaging of the backscatter signal is assumed. Signal integration for longer times should substantially increase range capability at the expense of time resolution.

Table 3. Estimates of Range (Height) for Determining Aerosol Concentration in Clear Air by 10.6-μm Lidar Systems*

Collecting Telescope Diam. (m)	Laser Transmitter Power (W)	Range (m) 10-m Ht.Resol.	20-m Ht.Resol.	50-m Ht.Resol.
0.1	10	60	—	—
0.3	10	180	250	400
0.3	50	300	450	700
0.3	100	400	600	900
0.3	300	550	850	1250
0.3	500	680	1000	1500

*Assumes a factor-of-2 fall-off in particle concentrations for each km of height

9. Conclusions

The test system described above afforded measurements of the backscatter signal during periods of enhanced local aerosol concentration. Determination of aerosol particle size distributions from Nuclepore filter samples permitted computation of anticipated backscatter. Comparison of the experimental and computed backscatter values shows agreement to within a factor of two. This is probably as good an agreement as can be expected in view of the fact that backscatter is dependent on the index of refraction of aerosol particles, which is known to differ for different types of aerosols. The backscatter results appear sufficiently representative to warrant their use in estimating the capabilities of backscatter lidar systems. The estimates given in the preceding section represent conservative values of lidar range for vertical sounding of aerosol concentrations in relatively clear air.

10. Acknowledgments

Dr. R. Pueschel and other staff members of the Atmospheric Physics and Chemistry Laboratory exposed and analyzed the aerosol filters that were used to calibrate the backscatter data. Their enthusiastic cooperation is much appreciated. The encouragement and guidance given by Dr. V. Derr during the course of the project are gratefully acknowledged.

11. References

Kerker, M. (1969): *The scattering of light, and other electromagnetic radiation.* Academic Press, N.Y. 1969.

McClatchey, R. A., R. W. Fenn, J. E. A. Selby, F. E. Boly, and J. S. Garing (1971): Optical properties of the atmosphere (revised). AFCRL–71–0279 (ERL Papers No. 354).

Pueschel, R., C. Van Valin and F. Parungo (1975): Effects of air pollutants on cloud nucleation. *Geophys. Res. Letters,* 1: 51–54.

Volz, F. E. (1972): Infrared refractive index of atmospheric aerosol substances. *Applied Optics,* 11:755–759.

Huffaker, R. M. (1974): CO_2 laser Doppler systems for the measurement of atmospheric winds and turbulence. *Atmospheric Technology* (NCAR), No. 6.

Schwiesow, R. L. and R. E. Cupp (1976): Remote Doppler velocity measurements of atmospheric dust devil vortices. *Applied Optics,* 15: 1–2.

Appendix I: Calibration Methods

Laser Beam Pattern

The manufacturer specifies the nominal beamwidth of the laser beam as <5 mrad and the exit beam diameter as <6 mm. Since the system calibration depends on the angular distribution of energy in the beam being known, it was deemed important to measure this distribution. A disc thermistor 2 mm in diameter was mounted on an X-Y translator at a distance of 5 m from the laser. The thermistor was connected to a battery and voltage divider, and a digital millivolt meter (DVM) was used to read the thermistor resistance. A change of 1°C resulted in about 50 mV change in the DVM. The laser beam was first sent through a CO_2 laser attenuator. With the attenuator set at minimum the thermistor was positioned near one edge of the laser beam, so its temperature was raised about 5° above the ambient temperature by the incident 10.6-μm energy. The translator was then used to move the thermistor in 2-mm steps across the beam. At each position, the attenuator was adjusted so the thermistor attained the same temperature after suitable settling time (~ 30 sec). The power out of the attentuator was measured after each adjustment. In this way a profile of relative power across the beam was obtained. It was found that the beam width was 3.0 ±0.2 mrad. The beam pattern was approximately Gaussian but had a center portion flatter than a true Gaussian curve.

Overall System Sensitivity

To provide a convenient check on overall sensitivity of the system, polished steel spheres of various diameters were positioned in the intersection volume of the transmitter and receiver beams. This method also provided a very convenient means of adjusting the beams during initial setup and ensuring that mechanical shifts had not occurred.

In the prototype system a ⅛-in-diameter sphere was positioned in the intersection volume, and both the transmitter and receiver beams were adjusted to obtain a maximum backscattered signal. Assuming that the beam pattern of the transmitter is known from the measurement described above, the power density incident on the sphere is known and backscatter intensity at the receiver mirror can be computed. This method was used periodically to check the system sensitivity. The repeatability of the measurement was within 10 percent.

Appendix II: Time-Share Program for Intersecting Beam Lidar System

A program called INTERSECTING BEAMS LIDAR was implemented on a time-share system. It requests input data that specify the system parameters, such as laser power, transmitter and receiver beamwidth, and system geometry. It assumes that the transmitter beam is initially directed perpendicular to the receiver beam and reflected from a mirror that can be rotated to sweep the laser beam along the receiving telescope beam. Figure 1 in the main text of this report schematically depicts the arrangement.

The program also requests input information on the concentration, size, and backscatter gain of target particles in the intersection volume. It then computes and outputs the geometrical parameters of the intersection volume and the backscatter signal for various ranges. These ranges are automatically incremented until the intersection volume has a length that exceeds a previously determined fraction of the range (typically 0.2).

A listing of the program is given below, followed by a sample calculation. Definitions of the input parameters have been inserted in parentheses on the sample calculation printout. The output values are: range in meters, from the receiving telescope to the intersection volume; the angular orientation of the steering mirror in degrees; the receiver beamwidth in radians; the width, length, and volume of the intersection volume; and the signal incident on the detector in watts.

Sample Program Run

```
Time-Share Program:   INTERSECTING BEAMS
                      LIDAR
Time-Share Language:  CAL

1.00 DEMAND P,R.D,A1,A2,D9,N9,A9,F,G1,A8

3.10 TYPE "
     DIAMETER OF PARTICLES "
6.06 SET D9=D9-(2E- 6)
6.07 TYPE D9
6.15 SET R=100
6.20 TO STEP 4.00

     RANGE  ANGLE  BMWDTH  WIDTH  LENGTH
      VOLUME  SIGNAL "
4.00 SET T=ATAN(D/R)
4.10 SET D2=D*(SIN(PI/4+T/2))/(SIN(.75
       *PI-T/2-A2/2))
4.15 SET R2=D2*(SIN(PI/2-T-A2))/SIN(T+A2/2)
4.20 SET D3+D*(SIN(.75*PI-T/2))/SIN
       (PI/4+T/2-A/2)
4.25 SET R3+D3*SIN(PI/2-T+A2)/SIN(T-A2/2)
4.30 SET S=R3-R2
4.35 SET W=P*A1
4.40 SET V=(PI/8)*A1*A1*(R3*R3+R2*R2)*
     (R3-R2)
4.50 SET R1=S/W
4.60 SET R4=S/R
5.05 TO STEP 6.05 IF R>13000
5.10 SET R9=D+SQRT(D*D+R*R)
5.15 TO STEP 6.05 IF (R3-R2)/R>.5
5.20 SET X=(P*4/(PI*A2*A2*R9*R9))
       *(D9*D9*PI*N9*V/4)*(A9*E*G1/(R*R
       *PI*4))*EXP(-(A8*R+A8*R9))
5.30 TYPE IN FORM
       1:R,(90-(T*180/PI))/2,A1,W,S,V,X
5.40 SET R=2*R
5.45 TO STEP 4.00

6.05 TYPE "

FORM 1:
%%%%% %%.%% %.%%%% #######
####### ######### #########

     /INTERSECTING

>TO PART 1

  P = 10      (Laser power output, in watts)
  R = 20      (Beginning range, in meters)
```

D = 1 (Distance between receiving beam and transmitter beam mirror, in meters)
A1 = .001 (Transmitted beamwidth, in radians)
A2 = .001 (Receiver beamwidth, in radians)
D9 = 1.5E–6 (Diameter of backscattering particles, in meters)
N9 = 1E6 (Concentration of particles, in part./m^3)
A9 = .07 (Receiving optics collection area, in m^2)
E = .6 (Optical system efficiency)
G1 = .0068 (Backscatter gain of particles)
A8 = .0002 (Attenuation coefficient of atmosphere, in neper/m)

RANGE	ANGLE	BMWDTH	WIDTH	VOLUME	SIGNAL	LENGTH
20	43.57	.0010	2.0–02	4.2–01	1.323–04	3.796–13
40	44.28	.0010	4.0–02	1.6 00	2.066–03	3.862–13
80	44.64	.0010	0.8–01	6.5 00	3.279–02	3.866–13
160	44.82	.0010	1.6–01	2.6 01	5.315–01	3.841–13
320	44.91	.0010	3.2–01	1.1 02	9.161 00	3.906–13

☆ U.S. GOVERNMENT PRINTING OFFICE: 1977–777–045–/1271

Environmental Research LABORATORIES

The mission of the Environmental Research Laboratories (ERL) is to conduct an integrated program of fundamental research, related technology development, and services to improve understanding and prediction of the geophysical environment comprising the oceans and inland waters, the lower and upper atmosphere, the space environment, and the Earth. The following participate in the ERL missions:

MESA *Marine EcoSystems Analysis Program.* Plans, directs, and coordinates the regional projects of NOAA and other federal agencies to assess the effect of ocean dumping, municipal and industrial waste discharge, deep ocean mining, and similar activities on marine ecosystems.

OCSEA *Outer Continental Shelf Environmental Assessment Program Office.* Plans and directs research studies supporting the assessment of the primary environmental impact of energy development along the outer continental shelf of Alaska; coordinates related research activities of federal, state, and private institutions.

WM *Weather Modification Program Office.* Plans, directs, and coordinates research within ERL relating to precipitation enhancement and mitigation of severe storms. Its National Hurricane and Experimental Meteorology Laboratory (NHEML) studies hurricane and tropical cumulus systems to experiment with methods for their beneficial modification and to develop techniques for better forecasting of tropical weather. The Research Facilities Center (RFC) maintains and operates aircraft and aircraft instrumentation for research programs of ERL and other government agencies.

AOML *Atlantic Oceanographic and Meteorological Laboratories.* Studies the physical, chemical, and geological characteristics and processes of the ocean waters, the sea floor, and the atmosphere above the ocean.

PMEL *Pacific Marine Environmental Laboratory.* Monitors and predicts the physical and biological effects of man's activities on Pacific Coast estuarine, coastal, deep-ocean, and near-shore marine environments.

GLERL *Great Lakes Environmental Research Laboratory.* Studies hydrology, waves, currents, lake levels, biological and chemical processes, and lake-air interaction in the Great Lakes and their watersheds; forecasts lake ice conditions.

GFDL *Geophysical Fluid Dynamics Laboratory.* Studies the dynamics of geophysical fluid systems (the atmosphere, the hydrosphere, and the cryosphere) through theoretical analysis and numerical simulation using powerful, high-speed digital computers.

APCL *Atmospheric Physics and Chemistry Laboratory.* Studies cloud and precipitation physics, chemical and particulate composition of the atmosphere, atmospheric electricity, and atmospheric heat transfer, with focus on developing methods of beneficial weather modification.

NSSL *National Severe Storms Laboratory.* Studies severe-storm circulation and dynamics, and develops techniques to detect and predict tornadoes, thunderstorms, and squall lines.

WPL *Wave Propagation Laboratory.* Studies the propagation of sound waves and electromagnetic waves at millimeter, infrared, and optical frequencies to develop new methods for remote measuring of the geophysical environment.

ARL *Air Resources Laboratories.* Studies the diffusion, transport, and dissipation of atmospheric pollutants; develops methods of predicting and controlling atmospheric pollution; monitors the global physical environment to detect climatic change.

AL *Aeronomy Laboratory.* Studies the physical and chemical processes of the stratosphere, ionosphere, and exosphere of the Earth and other planets, and their effect on high-altitude meteorological phenomena.

SEL *Space Environment Laboratory.* Studies solar-terrestrial physics (interplanetary, magnetospheric, and ionospheric); develops techniques for forecasting solar disturbances; provides real-time monitoring and forecasting of the space environment.

U.S. DEPARTMENT OF COMMERCE
National Oceanic and Atmospheric Administration
BOULDER, COLORADO 80302